

# Flexural behavior of the reinforced t-beam containing hybrid recycled-aggregate self-compacting concrete

Zhino A. Shawais<sup>1,a</sup>, Khamees N. Abdulhaleem<sup>1,b</sup>, Hussein Hamada<sup>2,c,\*</sup>

<sup>1</sup>Civil Engineering Department, University of Kirkuk, Kirkuk, Iraq

<sup>2</sup>Al-Qalam University College, Kirkuk 36001, Iraq

## Article Info

## Abstract

### Article History:

Received 04 Sep 2024

Accepted 06 Oct 2024

### Keywords:

Flexural behavior;  
T-Beam;  
Hybrid concrete;  
Recycled aggregate;  
Self-compacting  
concrete

Self-compacting concrete (SCC) flows under its weight and resists segregation, distinguishing it from conventional concrete. Recycled concrete aggregate (RCA) offers a sustainable alternative to natural aggregates, reducing resource depletion and enhancing environmental properties. This study experimentally investigates the flexural behavior of nine T-beams composed of hybrid SCC with varying reinforcement ratios ( $\rho_1 = 0.45\%$ ,  $\rho_2 = 1.05\%$ ,  $\rho_3 = 1.85\%$ ) and different RCA proportions (0%, 50%, 100%) in the web zone. At the same time, the flange was cast using only SCC. Four-point load tests were conducted to assess the impact of RCA replacement and reinforcement on the beams' performance. Results indicate that RCA replacement reduces the drop in loading capacity with increased reinforcement, improving both stiffness and bearing capacity. Additionally, higher RCA content shifted the failure mode from flexural to shear, particularly in beams with higher reinforcement ratios, demonstrating RCA use's economic and environmental benefits.

© 2024 MIM Research Group. All rights reserved.

## 1. Introduction

Self-compacting concrete (SCC) was first developed in Japan in 1988 to enhance concrete performance and increase durability [1]. This type of concrete offers various economic, social, and environmental benefits, including faster construction and reduced noise [2]. SCC is characterized by its ability to flow under its weight, allowing it to fill densely reinforced areas without segregation and without the need for vibrators [3-5]. Xiao [6] noted that incorporating recycled concrete aggregates (RCA) into concrete production presents an innovative solution to the global challenges of depleting natural resources. Sun et al. [7] evaluated the potential of using waste concrete recycling materials (WCRM) in SCC production. They replaced fine and coarse aggregates at varying levels while maintaining a constant water-binder ratio of 0.4. Their findings indicated that WCRM can reduce the strength and workability of SCC. Additionally, Xiao et al. [8] investigated the long-term effects of RCA on strength, shrinkage, and durability. They concluded that the long-term performance of RAC can improve over time.

Currently, there is a global trend towards developing innovative types of concrete to reduce pollution as well as reduce construction costs [9-11]. Therefore, sustainable and recyclable materials should be prioritized across various construction applications. One of the most practical and eco-friendly solutions is to repurpose concrete from the rubble of buildings demolished due to age or natural disasters. This approach provides an alternative to natural aggregates, helping to conserve natural resources commonly used in the construction industry [12]. Additionally, the use of industrial [13] and agricultural waste [14] further contributes to reducing resource depletion.

\*Corresponding author: [enghu76@gmail.com](mailto:enghu76@gmail.com)

<sup>a</sup>orcid.org/0009-0002-2178-6930; <sup>b</sup>orcid.org/0000-0001-9049-227X, <sup>c</sup>orcid.org/0000-0001-9911-8639

DOI: <http://dx.doi.org/10.17515/resm2024.428me0904rs>

Res. Eng. Struct. Mat. Vol. x Iss. x (xxxx) xx-xx

To produce economical and environmentally friendly concrete that meets specifications, materials with specific properties tailored to their position within the structural member can be used [4, 15, 16]. To enhance the efficiency of concrete, including reducing its weight and production cost, hybrid concrete (HC) can be utilized [17]. In structural members subjected to flexural loading, two behavior zones exist: one under tension and one under compression. Since reinforcing steel strengthens the tension zone, hybrid concrete containing recycled aggregate can be effectively employed in this region [18]. T-beams, commonly used in bridge decks and to support concrete slabs on simple walls, are ideal for large spans, making them suitable for industrial and commercial structures. They are also frequently used as precast members. One key advantage of T-beams is their large compression area, which increases the load-bearing capacity of the structural member [19].

Fahmy and Idriss [20] examined the flexural behavior of reinforced concrete T-beams made from hybrid concrete, incorporating recycled aggregate concrete (RAC) with both normal and high-strength concrete. Their results indicated that using RAC as a filler in the core of T-beam webs is a promising construction technique. It can effectively predict the development, propagation, and width of shear and flexural cracks. Hason et al. [17] evaluated the flexural ductility indices of T-beams made from natural aggregate (NA) and recycled aggregate (RA). They found that replacing NA with RA slightly reduced the flexural capacity and led to a decrease in the ductility indices of RA T-beams compared to reference beams.

Ali and Malik [21] conducted both experimental and theoretical investigations into the flexural and shear behavior of reinforced concrete T-beams made with hybrid concrete. Their findings highlighted the significant impact of using steel fibers in the web concrete and high-strength concrete in the flange, which resulted in increased maximum load and first cracking load. Fang et al. [22] studied the shear behavior of hybrid T-beams composed of lightweight and normal-weight concrete. They developed an equation to predict the interfacial shear transfer strength of these hybrid T-beams. Marzoq and Borhan [23] investigated the structural response of hybrid reinforced concrete T-beams made from reactive powder concrete (RPC) and normal concrete (NC) under bending moments. Testing four beams with different concrete types for the flange and web, they concluded that the type of concrete significantly influences T-beam behavior. You et al. [18] conducted an experimental study on self-compacting, simply supported hybrid fiber-reinforced concrete T-beams under four-point loading. Their results showed that hybrid fibers significantly enhanced the ultimate load and altered the failure mode.

Khattar and Khadir [19] studied the flexural behavior of T-beams cast from self-compacting concrete (SCC) with recycled coarse aggregate (RCA) partially replacing natural coarse aggregate at ratios of 0%, 50%, and 75%. They found that increasing the RCA replacement to 50% reduced the first cracking load by 15.5%, without affecting the ultimate load. At a 75% RCA replacement, both the first cracking load and ultimate load decreased by 31% and 10%, respectively, while deflection and crack width increased. Doubling the main reinforcement ratio led to a 20% increase in the first cracking load and a 46% increase in the ultimate load, with corresponding decreases in deflection and crack width.

Given the limited research on the structural behavior of hybrid concrete T-beams incorporating self-compacting concrete (SCC), this study focuses on the flexural performance of such beams made with SCC using either natural coarse aggregate (NCA) or recycled coarse aggregate (RCA). The coarse aggregate in the web zone was replaced by 0%, 50%, and 100%, resulting in three groups of T-beams. Each group was further tested with three different main reinforcement diameters (8mm, 12mm, 16mm) to assess their impact on the beams' flexural behavior. This research aims to deepen the understanding of reinforced concrete with RCA and serves as a valuable reference for both future studies and practical engineering applications involving RAC.

## **2. Experimental Program**

This study presents the details of the experimental program, including a brief description of the material properties and quantities used in the concrete mixtures. It also outlines the specimens utilized to investigate the flexural behavior of reinforced concrete T-beams. The production

method of self-compacting concrete (SCC) and the tests conducted on both its fresh and hardened states are briefly reviewed. Additionally, the testing procedures for the T-beams and the mechanisms used to evaluate their behavior are thoroughly explained.

Three different concrete mixtures were prepared, each with varying proportions of recycled coarse aggregate (0%, 50%, and 100%) replacing natural coarse aggregate (NCA). For each mixture, three concrete beams were cast with main reinforcement steel of varying diameters (8mm, 12mm, and 16mm) in the tension zone. The three mixtures were used for casting the web zone, while the mixture containing only NCA was applied to the flange zone of the concrete T-beams.

## 2.1. Materials Description

### 2.1.1 Cement

Ordinary Portland cement was used in this study, with a fineness modulus of 295 m<sup>2</sup>/kg and a specific gravity of 3.15 which is locally manufactured and complies with the approved standards and specifications [24].

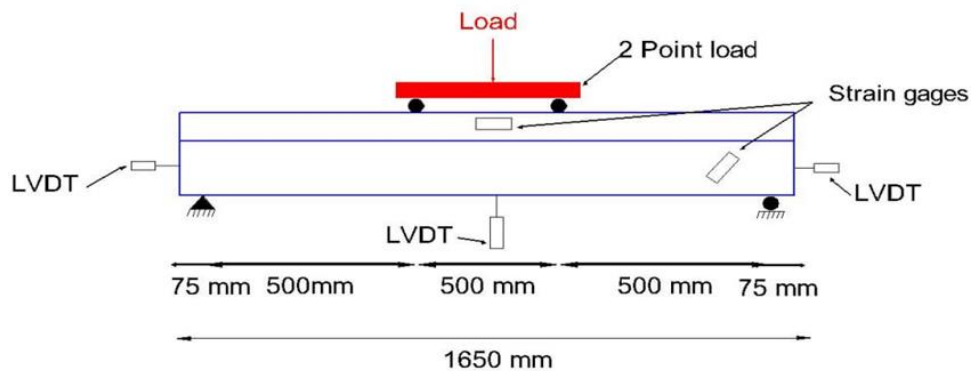


Fig. 1. Illustration of the dimensions and details of the T-beam specimens

### 2.1.2 Fly Ash

About 7% of the world's carbon dioxide emissions come from the production process of ordinary Portland cement (OPC) [25], so fly ash (class F) with a specific gravity of 2.2 was used as a binder and filler to reduce the amount of cement used and produce SCC that complies with the specifications.

### 2.1.3 Silica Fume

Since silica fume contains a high percentage of silicate oxide, it is added to concrete to increase its compressive strength through its reaction with calcium hydroxide. The chemical components and their proportions for cement, fly ash, and silica fume are listed in Table 1.

Table 1. The chemical components of the cement, fly ash, and silica fume.

Oxide (%)	Cement	Fly ash	Silica fume
CaO	62.6	5.11	0.4
Al <sub>2</sub> O <sub>3</sub>	5.03	20.73	0.7
SiO <sub>2</sub>	20.77	55.67	93.2
MgO	2.3	2.65	0.1
Fe <sub>2</sub> O <sub>3</sub>	3.1	12.96	1.5
K <sub>2</sub> O +Na <sub>2</sub> O	1.08	2.54	1.4
SO <sub>3</sub>	2.16	0.34	0.1
Specific gravity	3.15	2.2	2.1

### 2.1.4 Fine and Normal Coarse Aggregates

The fine and natural coarse aggregates (NCA) used in the study were locally sourced, river-rounded aggregates that conformed to the specifications outlined in [26]. The fineness modulus of the fine aggregate was 2.34, with a maximum coarse aggregate size of 16 mm. The water absorption rates for the fine and coarse aggregates were 2.1% and 0.57%, respectively, while their specific gravities were 2.58 and 2.65. Detailed sieve analyses for both fine and coarse aggregates are presented in Tables 2 and 3, respectively.

### 2.1.5 Recycled Coarse Aggregate (RCA)

The main objective of the present study is to replace the NCA with RCA. The source of the RCA is the rubble of the concrete roof of a demolished house whose age is more than 25 years. The concrete blocks were brought to the laboratory and crushed, after which sieve analysis was conducted to obtain aggregates with acceptable gradation. To ensure obtaining RCA with gradation identical to the NCA, the recycled aggregate of each size was stored in special bags. Then, the aggregates were used in the required weights according to the gradation ratio as inserted in Table (3). The specific gravity of the RCA was 2.45, while its water absorption rate was 5.7%. The physical properties of RCA as shown in Table 4.

Table 2. Sieve analysis of fine aggregate

Sieve No.	Passing%	ASTM Standard Limits [26].
3/8 in (9.5 mm)	100	100
No.4 (4.75mm)	98	90-100
No.8 (2.36mm)	92	75-100
No.16 (1.18mm)	81	55-90
No.30 (0.6mm)	58	35-59
No.50 (0.3mm)	26	8-30
No.100 (0.15mm)	7	0-10
Sieve No.	Passing %	ASTM Standard Limits [26].

Table 3. Sieve analysis of NCA and RCA

Sieve Size (mm)	Percentage of Passing		ASTM Standard Limits [26]
	NCA	RCA	
20	100	100	100
14	94	94	90 -100
10	62	62	50 - 85
5	0	0	0 - 10

Table 4. Physical properties of RCA

Dry Specific gravity	2.27
SSD Specific gravity	2.4
Apparent Specific gravity	2.45
Loose bulk density	1481 kg/m <sup>3</sup>
Rodded bulk density	1594 kg/m <sup>3</sup>
Water absorption	5.7 %

### 2.1.6 Super-Plasticizer

To ensure that SCC according to the specifications, a superplasticizer (SP) was added to the concrete mixtures at a rate of 1.5 % to improve its flowability and fluidity. Viscocrete GS-180, which was produced by Sika for additives, was used. This superplasticizer helps to reduce the amount of water in the mixture and increase its viscosity.

### 2.1.7 Steel Reinforcement

To study the effect of changing the area of reinforcement on the behavior of concrete T-beams, three different diameters of steel were used for the main reinforcement (longitudinal direction) in the tension zone. Reinforcement bars with diameters (8mm, 12mm, and 16mm) were used, with reinforcement ratios (0.45%, 1.05%, and 1.85%), respectively. On the other hand, reinforcement bars with a diameter (8 mm) were used for the shear reinforcement (stirrups) of all concrete beams to resist the shear stresses. The physical properties of the reinforcing bars used in the present study are listed in Table 5.

Table 5. Physical properties of the steel reinforcing bar

Bar diameter (mm)	Yield strength F <sub>y</sub> (MPa)	Ultimate stress F <sub>u</sub> (MPa)
8	388	552
12	544	645
16	568	652

### 2.2 Mixing Proportions

The design of SCC mixes is different from that of conventional concrete. Trial and error are used to determine the proportions of concrete mix materials using EFNARC limitations [27]. Three basic criteria must be satisfied to produce an SCC that meets the specifications: including the ability to flow without vibrating and its resistance to segregation. Consequently, the fresh properties of concrete used in the present study are determined through basic tests, including slump flow test, V-funnel test, and L-box test. These tests are subject to EFNARC specifications and guidelines [27]. According to these tests, the proportions of materials for concrete mixes were determined. The NCA was replaced by RCA in three proportions (0%, 50%, and 100%). The water-to-binder ratio (w/b) and superplasticizer content for all concrete mixtures were 0.4 and 1.5%, respectively. We maintained a consistent water-cement ratio for all concrete mixtures. When adjusting the RCA content from 0% to 50% and then to 100%, was added extra water based on the RCA's absorption rate to preserve the water-binder ratio across the three mixtures. This additional water ensures the RCA reaches a saturated surface-dry (SSD) condition without affecting the absorption rate of the SCC mix. The quantities of materials used in the concrete mixes for the present study are listed in Table 6.

Table 6. The concrete design mixes used in the present study

Materials	Mix Code		
	SCC-RC00	SCC-RC50	SCC-RC100
Cement (kg/m <sup>3</sup> )	370	370	370
Fly Ash (kg/m <sup>3</sup> )	80	80	80
Silica Fume (kg/m <sup>3</sup> )	50	50	50
Water (l/m <sup>3</sup> )	200	200	200
Water/Cement (w/c)	0.54	0.54	0.54
Water/Binder (w/b)	0.4	0.4	0.4
Superplasticizer (%)	1.5	1.5	1.5
Fine Aggregate (kg/m <sup>3</sup> )	800	800	800
NCA (kg/m <sup>3</sup> )	850	425	0
RCA (kg/m <sup>3</sup> )	0	393	786

### 2.3 T-Beam Designation

The T-beam specimens were designed with appropriate dimensions to simulate real structural members, providing an accurate representation of their behavior under applied loads. In the laboratory, the T-beams measured 1650 mm in total length and 250 mm in total depth. The flange was 60 mm thick and 200 mm wide. The web of the T-beam was 100 mm wide with a clear height of 190 mm, as illustrated in Figure 1. Flexural behavior was analyzed by applying two-point loads after dividing the clear span into three equal parts, ensuring a shear-to-span ratio of 2. The clear



span between supports was 1500 mm for each specimen. After manufacturing the molds with the specified dimensions, they were painted before pouring the concrete to ensure easy demolding and smooth specimen surfaces. The main reinforcement bars and shear reinforcement were prepared according to the specified dimensions for each specimen. Additionally, the concrete mix components were weighed and prepared with precision, following the quantity schedule, before the pouring process. A concrete cover of 15 mm was maintained from all directions for all T-beams.

### 2.4 Specimen Preparation

To investigate the flexural behavior of T-beam specimens, the experimental program involves preparing and casting nine distinct T-beam specimens made from hybrid self-compacting concrete (SCC). The study examines the impact of varying the main reinforcement area on flexural behavior by using three different diameters for the tension zone: 8 mm, 12 mm, and 16 mm, represented as 2Ø8, 2Ø12, and 2Ø16, respectively. For each reinforcement type, three concrete mixtures were utilized: SCC-RC00, SCC-RC50, and SCC-RC100.

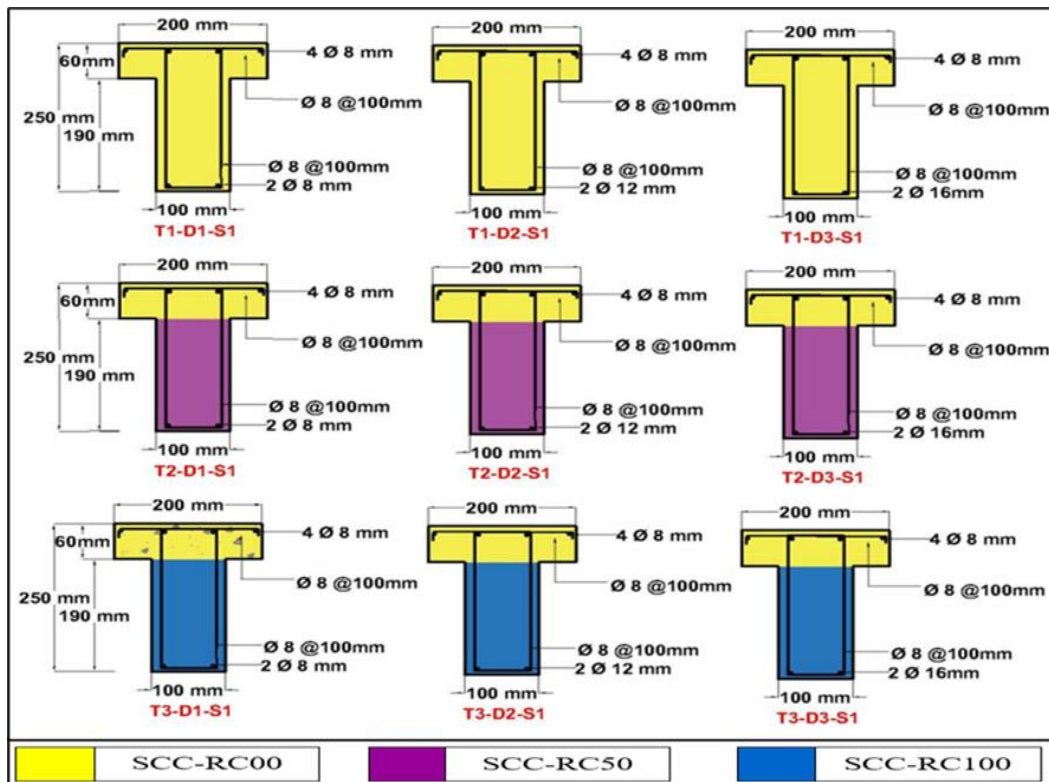


Fig. 2. The details illustration of the T-beam specimens used in the present study

Table 7. Classification of the T-beam specimens

T-beam code	Concrete type in T-beam web.	Concrete type in T-beam flange.	Main reinforcement
T1-D1			2Ø8
T1-D2	SCC-RC00 <sup>1</sup>		2Ø12
T1-D3			2Ø16
T2-D1			2Ø8
T2-D2	SCC-RC50 <sup>2</sup>	SCC-RC00 <sup>1</sup>	2Ø12
T2-D3			2Ø16
T3-D1			2Ø8
T3-D2	SCC-RC100 <sup>3</sup>		2Ø12
T3-D3			2Ø16

1: SCC mixture 0% RCA, 2: SCC mixture 50% RCA, 3: SCC mixture 100% RCA.

The first mixture, SCC-RC00, consists of pure SCC without any replacement of natural coarse aggregate (NCA). In the second mixture, SCC-RC50, 50% of the NCA was replaced with recycled concrete aggregate (RCA) in the web, while the flange was cast using SCC-RC00. The third mixture, SCC-RC100, involved a complete replacement of NCA with RCA, applied to all three reinforcement types. To maintain consistent flexural behavior across all T-beams, the spacing of the shear reinforcement (stirrups) was kept constant at  $\emptyset 8@100$  mm. The T-beam specimens are classified and grouped as shown in Table 7. Figure 2 illustrates the details of the reinforcements and the types of concrete used for casting the flange and web of the T-beams.

## 2.5 Mixture Preparation and Casting

The preparation method for self-consolidating concrete (SCC) differs from that of conventional concrete. The materials listed in Table 7 are used to calculate the quantities required for one batch. First, the coarse and fine aggregates are mixed with additional water for two minutes to achieve a saturated surface dry (SSD) condition. Next, the binder materials cement, fly ash, and silica fume are added along with half the water volume, and this mixture is blended for another two minutes. The remaining water is combined with the superplasticizer and incorporated into the mixture. Mixing continues for five minutes to ensure uniformity.

Once the mixing is complete, immediate fresh tests are conducted on the SCC mixture to assess its properties. Three tests are performed: the slump flow test, V-funnel test, and L-box test. The T-beam models are then cast according to the specified details, along with three cubes and three cylinders for each concrete batch, without the use of a vibrator. Only the web zone of each T-beam specimen is cast initially. After 24 hours, the flange zone is cast using SCC containing only normal coarse aggregate (NCA). Following another 24 hours, the specimens are removed and immersed in water for curing for 28 days before testing.

## 2.6 Testing Procedures

Since the concrete used is self-compacting, it was necessary to conduct fresh tests for each concrete mixture in its fresh state. Also, the compressive strength and tensile strength of the concrete in its hardened state will be found. On the other hand, the flexural test of reinforced concrete T-beams will be conducted to know the flexural behavior.

### 2.6.1 Fresh Properties Testing

The fresh properties of the mixtures used in this study were assessed according to EFNARC specifications. To evaluate flowability and viscosity, the slump flow test was conducted. The V-funnel test was employed to determine the filling ability of the self-compacting concrete (SCC). Additionally, the L-box test was used to assess the concrete's resistance to segregation.

In the slump test, the time taken for the concrete to reach the circumference of a circle with a diameter of 500 mm is recorded after lifting the cone. The final diameter of the circular area resulting from the spread of the concrete, known as the slump diameter, is also measured. Following this, the V-shaped funnel flow test is conducted, where the time taken for the mixture to completely empty the funnel is recorded. Finally, the L-box test measures the vertical distances at the start ( $h_1$ ) and end ( $h_2$ ) of the basin after the concrete flow ceases, allowing for the calculation of the  $h_2/h_1$  ratio.

### 2.6.2 Hardened Properties Testing

The compressive strength and tensile strength of concrete used in the present study will be determined by mechanical tests at 28 days of age. A 2000 kN universal testing machine will be used. The compressive strength of each concrete mixture will be determined using cubic specimens of size 100\*100\*100 mm. The cubic specimens were loaded at a rate of 0.3 MPa/s according to British Standard (B.S) [28]. Also, the splitting test will be conducted for cylindrical specimens of size 100\*200 mm, according to ASTM [29]. The cylindrical specimens are loaded at a rate of 1.5 kN/s. To obtain reasonable results, the average strength value of three identical specimens will be found.

### 2.6.3 Flexural Testing

After 28 days of curing in water, the specimens will be removed, and their surfaces will be thoroughly cleaned. They will then be painted white to enhance the visibility of cracks and their progression during loading. A strain gauge will be affixed horizontally above the expected failure line (the beam's midpoint) to measure the concrete strain under flexural behavior. Additionally, another strain gauge will be attached along the line connecting the support and loading location at a 45-degree angle on both sides of the T-beam to assess the shear behavior during loading.

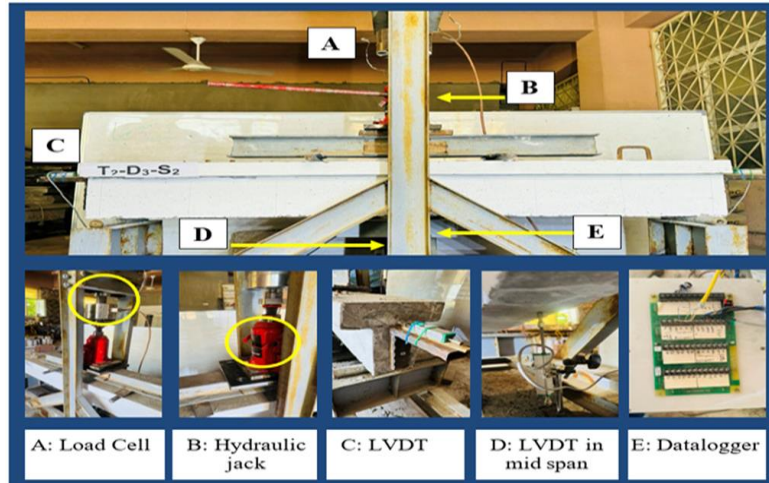


Fig. 3. Illustrations of the concrete T-beam testing procedure

To measure deflection under loading, a linear variable displacement transducer (LVDT) will be installed at the mid-span of the beam from the bottom, with an accuracy of approximately 75/4000 mm. Two additional LVDTs, each with an accuracy of about 25/4000 mm, will be positioned on both sides of the specimen (in the web zone) to measure horizontal displacement (slip) from each side of the T-beam. These instruments will be connected to an 80-rpm data logger, which in turn will be linked to a laptop. The specimens will be subjected to loading using a 200 kN load cell. For each loading stage, the loads and corresponding deflections on the beam surface will be recorded, along with observations of cracks until the test concludes. Loading will cease when the deflection reaches 30 mm for all T-beam specimens. The data on loads and deflection results will be automatically saved on the computer. After completing the test, photographs of the specimen, crack patterns, and the final failure form will be taken. Figure 3 illustrates the steps involved in performing the load test on the T-beam specimens.

## 3. Results and Discussion

### 3.1 Fresh Properties of SCC

The fresh properties of the SCC mixtures were evaluated through three tests to ensure compliance with EFNARC specifications. A slump flow test measured the concrete's flowability, a V-funnel test assessed its flow time, and an L-box test examined its resistance to segregation.

Table 8. Results of fresh properties of SCC mixtures

Mix Code	RCA %	Slump Test		V-funnel sec.	L-Box ( $h_2/h_1$ )
		$T_{500}$ (sec.)	Dia (mm)		
SCC-RC00	0%	2.34	760	6.72	0.94
SCC-RC50	50%	2.84	744	8.55	0.91
SCC-RC100	100%	3.32	720	10.53	0.88
EFNARC limitations [4].		2-5	600-800	$\leq 12$	0.8-1.0

According to EFNARC, the slump flow time ( $T_{500}$ ) should range between 2 and 5 seconds, with the flow diameter ideally between 600 and 800 mm. The V-funnel flow time should not exceed 12



seconds, and the L-box ratio ( $h_2/h_1$ ) should fall between 0.8 and 1. The test results of the mixtures used in this study, shown in Table 8, were consistent with EFNARC standards. The T500 for all mixtures was under 5 seconds, while the slump flow diameters ranged from 720 to 760 mm. V-funnel flow times ranged between 6.72 and 10.53 seconds, and the L-box ratio ( $h_2/h_1$ ) was between 0.88 and 0.94. Overall, all mixtures adhered to EFNARC specifications.

### 3.2 Hardened Properties of SCC Mixtures

The compressive and tensile strengths of the concrete used in this study are presented in Table 9. These values represent the average of three specimens for each concrete mixture. The results indicate that compressive and tensile strengths gradually decreased as the percentage of RCA replacement increased, compared to the mixture containing only NCA. Specifically, compressive strength decreased by 9% and 25%, and tensile strength by 28% and 39%, respectively, for 50% and 100% RCA replacement, as detailed in Table 9. This reduction in strength can be attributed to the lower quality of RCA compared to NCA, as the RCA was sourced from construction rubble specifically, the demolition of a house roof over 25 years old. Additionally, the brittleness of the aggregate was likely exacerbated by the crushing process used to obtain coarse aggregates of the required size and specification.

Table 9. Results of Hardened properties of SCC mixtures

Mix Code	RCA %	Compressive strength (MPa)	Tensile strength (MPa)
SCC-RC00	0	67.0	5.93
SCC-RC50	50	61.1	4.26
SCC-RC100	100	50.4	3.63

### 3.3 Flexural Behavior of T-Beam

The flexural test results for T-beams reveal their general behavior under flexural loading, summarized as follows: In the early stages, initial cracks appear in the lower portion of the mid-span tensile zone. The load at which these cracks first form is known as the first cracking load ( $P_{cr}$ ). As the load increases, these cracks widen and spread until the yield load ( $P_y$ ) is reached, marking the onset of reinforcement steel yielding. Beyond this point, deflection rises rapidly while load capacity slows, reaching the ultimate load ( $P_u$ ). Afterward, the load capacity decreases as deflection continues to increase, eventually leading to beam failure. Table 10 presents the test results, showing the load values along with corresponding deflections for the T-beams.

Table 10. Flexural test results for concrete T-beams used in the present study

T-beam code	First cracking point		Yielding point		Ultimate point		Ductility index $\Delta u/\Delta y$	stiffness $(KN/m) / \Delta y$	Failure mode*
	Load ( $P_{cr}$ ) (kN)	Deflection ( $\Delta cr$ ) (mm)	Load ( $P_y$ ) (kN)	Deflection ( $\Delta y$ ) (mm)	Load ( $P_u$ ) (kN)	Deflection ( $\Delta u$ ) (mm)			
T1-D1	16.6	1.51	37.4	5.19	54.1	30	5.78	7.21	F
T1-D2	29.4	1.89	126.1	13.75	143.2	30	2.18	9.17	F+S
T1-D3	30.9	2.09	181.9	14.71	198.9	30	2.04	12.37	F+S
T2-D1	16.4	1.08	37.7	5.76	44.1	30	5.21	6.55	F
T2-D2	19.9	1.66	132.5	13.61	135.2	30	2.20	9.74	F+S
T2-D3	28.8	2.01	173.1	13.11	185.3	30	2.29	13.20	F+S
T3-D1	15.3	1.66	24.8	5.06	42.5	30	5.93	4.90	F
T3-D2	17.6	1.24	120.9	11.49	129.1	30	2.61	10.52	S
T3-D3	19.2	1.43	174.3	10.53	174.4	15.89	1.51	16.55	S

\* F: Flexural failure, S: Shear failure.

#### 3.3.1 Load Capacity

Table 10 presents the load-capacity stages of concrete T-beams with varying replacement ratios of RCA (0%, 50%, and 100%) and three different reinforcement ratios (0.45%, 1.05%, and 1.85%). The first cracking load was observed to increase as the RCA replacement ratio rose, regardless of

the reinforcement ratio. This suggests a reduction in the stiffness of the T-beam with higher RCA content, as illustrated in Figure 4. Overall, the yielding load of the T-beam increases with a larger reinforcement area but decreases as the RCA replacement ratio increases. For concrete with NCA, the yielding load increased by 237% and 386%, corresponding to reinforcement ratio increases of 233% and 311%, respectively. When 50% of the NCA was replaced with RCA, the yielding load increased by 252% and 360% for the same reinforcement increases. Replacing all the NCA with RCA resulted in even higher increases in yielding load, by 388% and 603%, for the same reinforcement ratio increments.

Conversely, when using 8 mm diameter reinforcing bars, the ultimate load decreased by 19% and 22% for RCA replacement ratios of 50% and 100%, respectively. With 12 mm diameter bars, the decrease in ultimate load was 6% and 10% for the same replacement ratios. For 16 mm diameter bars, the reductions were 7% and 12%, respectively, for 50% and 100% RCA replacement. In conclusion, the reduction in load capacity of concrete T-beams decreases as the RCA replacement ratio increases, especially with higher reinforcement ratios. This indicates that using RCA in the web of concrete not only improves load capacity but also offers economic and environmental benefits compared to NCA.

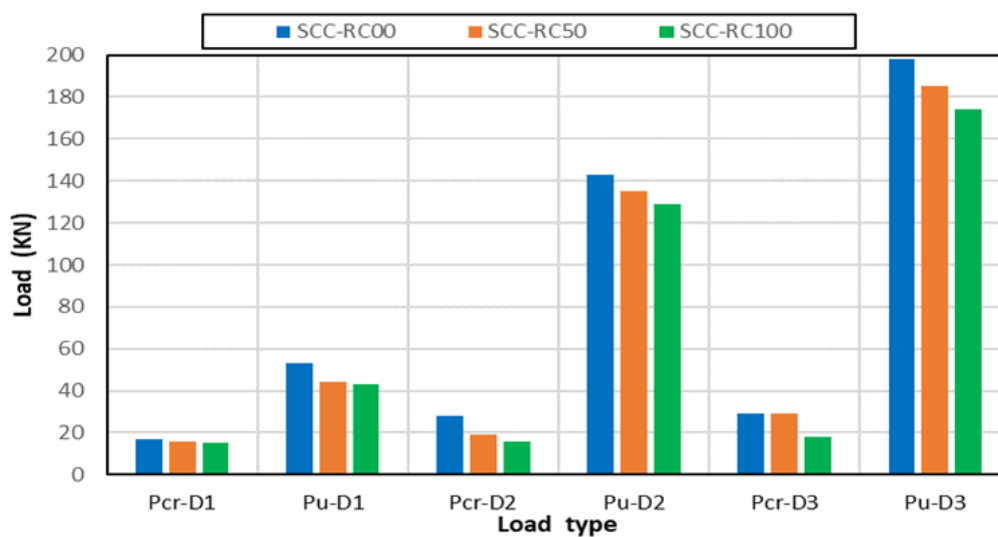


Fig. 4. Comparison between the first cracking load and the ultimate load of the T-beam specimens

### 3.3.2 Load-Deflection Curves

The flexural load test on the concrete T-beams was applied gradually until failure. At each loading stage, the deflection at the mid-span of the beam was recorded using LVDT, with the load being measured by an installed load cell. The load and deflection data were automatically saved on the computer in real-time. The study will examine the impact of different concrete types in the T-beam web and varying proportions of steel reinforcement on the load-deflection curves of each beam. In the graphs, the horizontal axis (X) represents deflection in millimeters (mm), while the vertical axis (Y) represents load in kilonewtons (kN).

#### • 3.3.2.1 Effect of Concrete Type

To investigate the effect of replacing natural coarse aggregate (NCA) with recycled coarse aggregate (RCA) in the concrete used for casting the web of T-beams, load-deflection curves were analyzed for each group. Figure 5 shows the load-deflection behavior of concrete beams with a reinforcement ratio of 0.45%, using different RCA replacement ratios (0%, 50%, 100%). The curves indicate that as the replacement ratio increases, the load-carrying capacity decreases with higher deflection, though all beams exhibited flexural behavior across the replacement ratios. In contrast, T-beams with a reinforcement ratio of 1.05% showed similar behavior regardless of whether NCA was replaced by RCA, with all beams maintaining flexural behavior, as depicted in Figure 6. For beams with a reinforcement ratio of 1.85%, shown in Figure 7, increasing the RCA replacement

ratio resulted in a shift from flexural to shear behavior. A full (100%) replacement of coarse aggregate weakened the concrete, altering the T-beam behavior from flexural to shear.

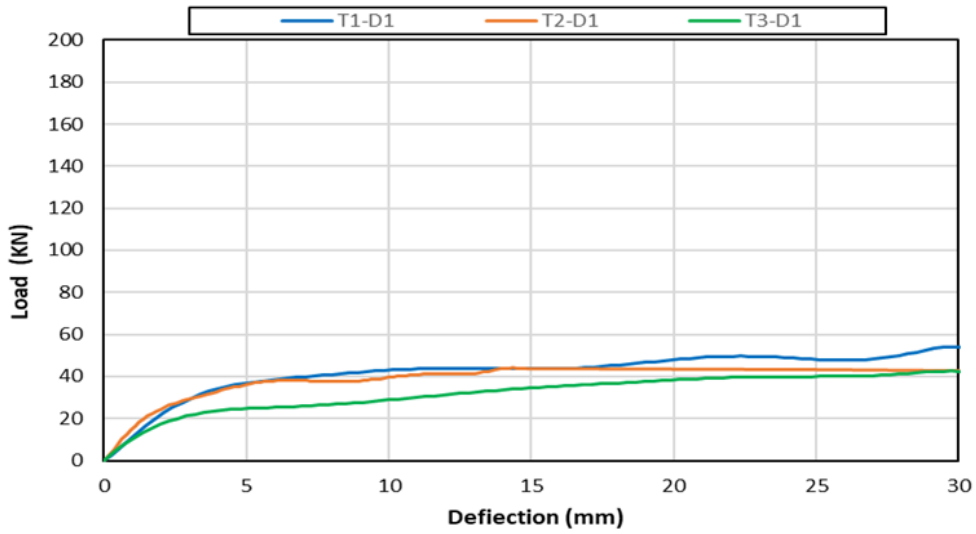


Fig. 5. Load-deflection curves for T-beams reinforced with steel bars of 8 mm

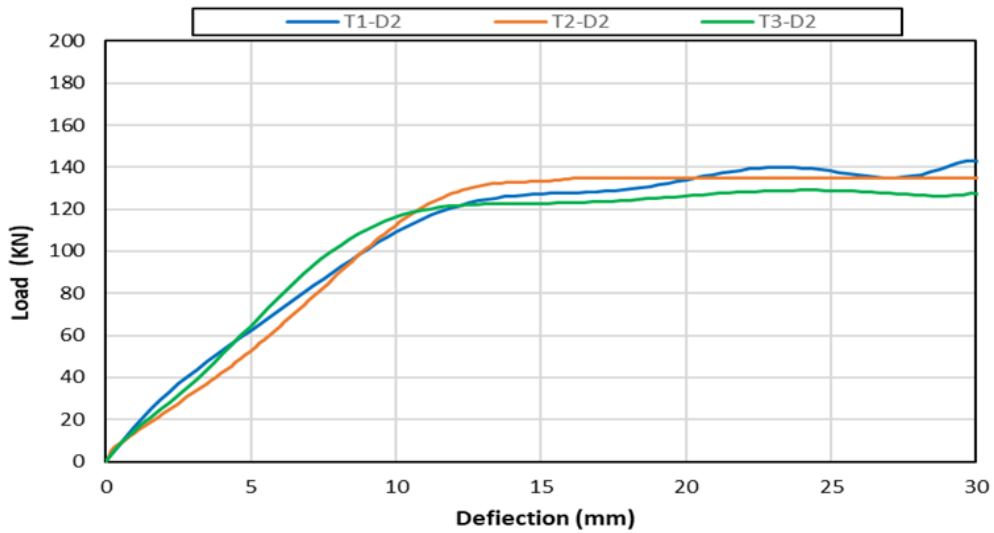


Fig. 6. Load-deflection curves for T-beams reinforced with steel bars of 12 mm

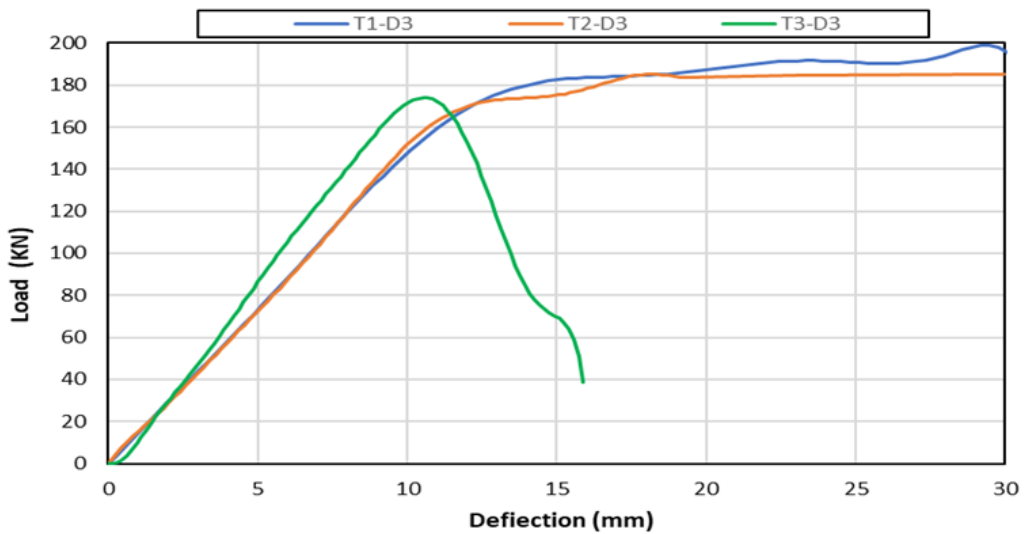


Fig. 7. Load-deflection curves for T-beams reinforced with steel bars of 16mm

• 3.3.2.2 Effect of Main Reinforcement

To investigate the impact of increasing the reinforcement ratio on the load-deflection behavior of concrete T-beams, Figure 8 illustrates the performance of T-beams made entirely with natural coarse aggregate (NCA) in both the flange and web, using three different reinforcement ratios (0.45%, 1.05%, and 1.85%).

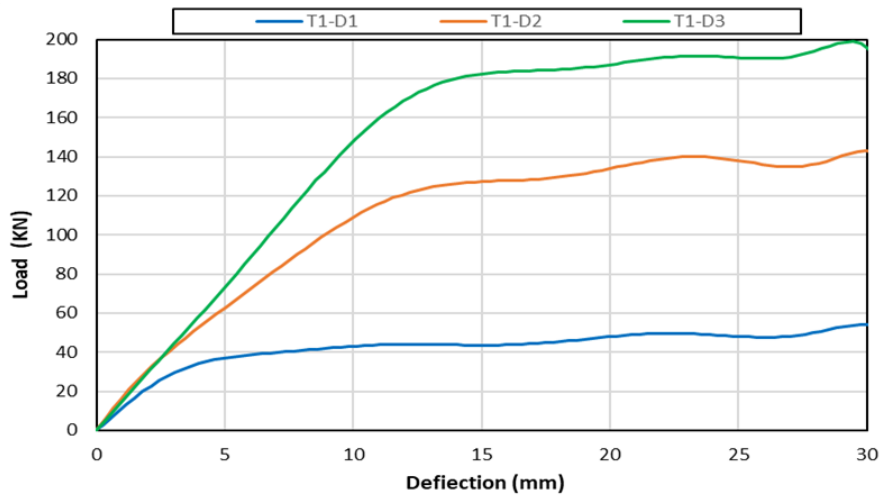


Fig. 8. Load-deflection curves for T-beams containing SCC-RC00 mixtures

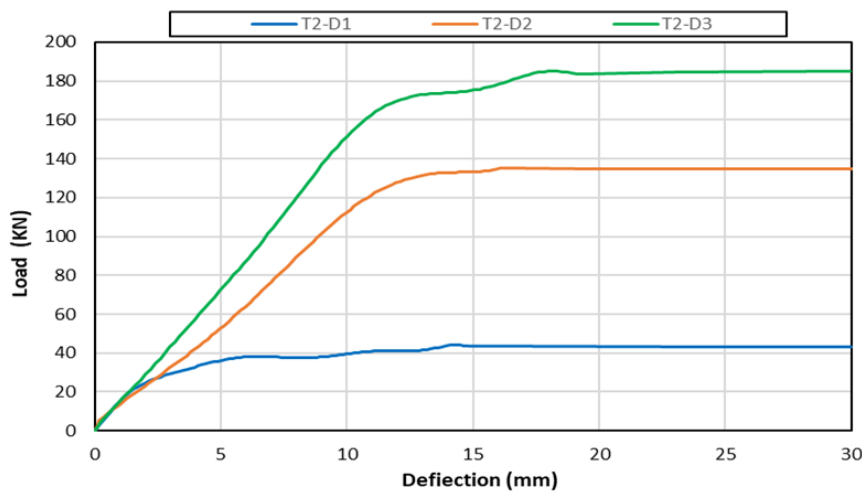


Fig. 9. Load-deflection curves for T-beams containing SCC-RC50 mixtures

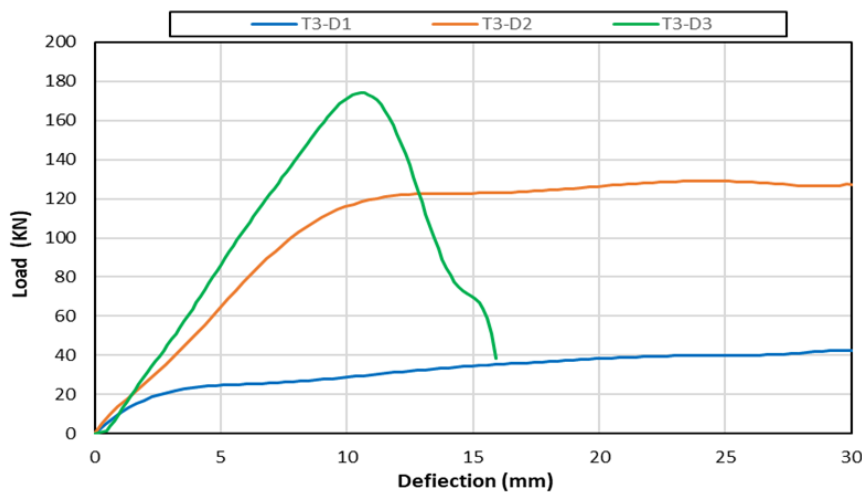


Fig. 10. Load-deflection curves for T-beams containing SCC-RC100 mixtures.

The use of NCA in the web's concrete helped preserve the flexural behavior of the T-beams, regardless of the steel reinforcement ratio. In contrast, replacing 50% of the natural aggregate with recycled coarse aggregate (RCA) partially maintains the flexural behavior of the beams, though the yield point is delayed as the reinforcement diameter increases, as shown in Figure 9. When 100% of the NCA in the web is replaced with RCA, the behavior of the T-beams gradually shifts from flexural to shear-dominant as the reinforcement ratio increases, as depicted in Figure 10.

### 3.3.3 Crack Patterns and Mod Failures

The failure patterns of concrete T-beams under loading are illustrated in Figures 11, 12, and 13. Vertical cracks initially develop from the middle of the beam's underside, resulting from a combination of flexural and shear failure. This effect becomes more pronounced as the percentage of recycled aggregate replacement increases. When using 16 mm diameter reinforcing steel, shear cracks appear alongside flexural cracks, and with higher aggregate replacement, shear cracks become more frequent until shear failure dominates, as shown in Figure 13.

Figure 11 highlights the failure modes of T-beams reinforced with 8 mm diameter bars, where flexural failure is predominant. Vertical cracks, concentrated in the beam's center, occur regardless of the aggregate replacement ratio. In contrast, Figure 12 shows the emergence of inclined cracks at a 45-degree angle in T-beams reinforced with 12 mm diameter bars. These inclined cracks appear alongside vertical cracks as the aggregate replacement ratio increases, resulting in a flexural-shear failure mode. As the main reinforcement ratio increases, the failure mode transitions from flexural-shear failure to pure shear failure, especially when coarse aggregate is fully replaced with recycled aggregate.



Fig. 11. Crack patterns and failure modes for T-beams reinforced with steel bar of 8 mm



Fig. 12. Crack patterns and failure modes for T-beams reinforced with steel bar of 12 mm



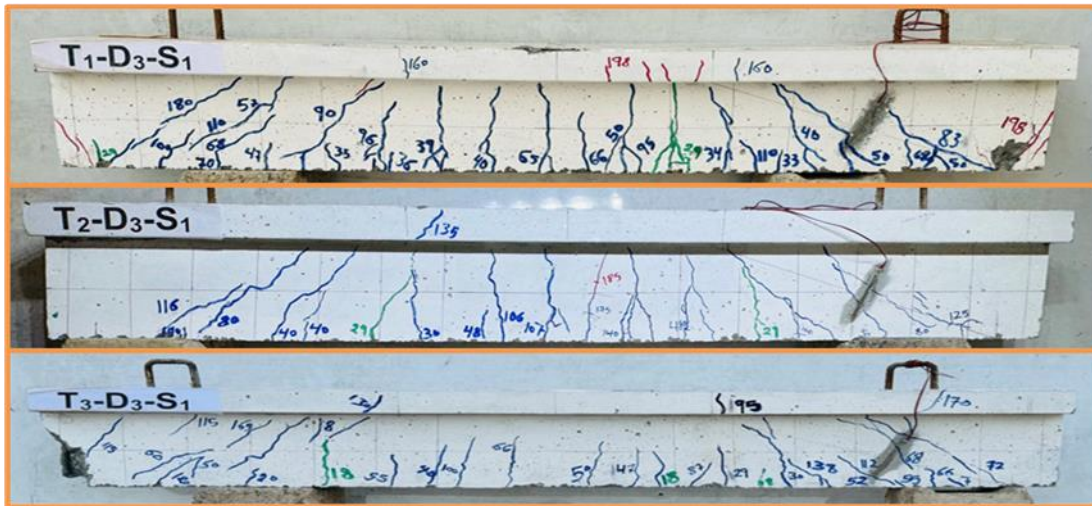


Fig. 13. Crack patterns and failure modes for T-beams reinforced with steel bar of 16 mm

### 3.3.4 Ductility Index

The ductility index measures a structural member's ability to withstand deformations without a substantial reduction in bending capacity. Several factors influence a member's deformability, such as the ratio of main reinforcement, the amount of secondary reinforcement, and the concrete strength [30]. The ductility index is expressed as the ratio of the deflection at ultimate load ( $\Delta_u$ ) to the deflection at yield point ( $\Delta_y$ ), as shown in Equation 1 [31]:

$$\text{Ductility index} = \Delta_u / \Delta_y \quad (1)$$

This equation was used to determine the ductility values of concrete beams by varying the ratios of the main reinforcement steel and the concrete strength. Generally, the ductility of concrete T-beams decreases as the steel reinforcement area increases, while the percentage of natural coarse aggregate (NCA) replacement remains constant. Additionally, increasing the replacement percentage of aggregates further reduces ductility, particularly in beams with a high reinforcement ratio.

### 3.3.5 Stiffness

Stiffness ( $K$ ) quantifies an elastic body's resistance to deformation. The effective section stiffness is determined by the maximum bearing force and the corresponding deflection within the service load zone (elastic zone) [32]. This relationship can be expressed mathematically as follows:

$$K = P_y / \Delta_y \quad (2)$$

In general, the stiffness of concrete T-beams increases with a higher percentage of main steel reinforcement, regardless of the level of aggregate replacement [33]. When beams are reinforced with 16 mm diameter bars instead of 8 mm bars, the stiffness increases by 72%, 102%, and 238% for coarse aggregate replacement percentages of 0%, 50%, and 100%, respectively. This trend highlights how increased steel reinforcement enhances a structural member's resistance to bending and deformation caused by external loads. Additionally, the results presented in Table 10 indicate that increasing the percentage of coarse aggregate replacement with recycled aggregate improves the stiffness of concrete beams. This improvement may be due to the recycled aggregate's initial resistance to loads; however, this resistance diminishes rapidly as the loading increases [34].

## 4. Conclusions and Recommendations

The current study examines how varying proportions of recycled concrete aggregate (RCA) and the reinforcing steel ratio affect the flexural behavior of hybrid T-beams in self-compacting concrete (SCC). The main conclusions are as follows:

- Replacing natural aggregates with RCA affects the workability of SCC, but it remains within the acceptable range defined by EFNARC guidelines.
- Increasing RCA replacement from 0% to 100% leads to a reduction in compressive strength, from 67.0 MPa to 50.4 MPa, and in splitting tensile strength, from 5.93 MPa to 3.63 MPa.
- The load capacity of reinforced concrete T-beams decreases with higher RCA replacement ratios; however, this reduction is mitigated by increasing the reinforcement ratio. This suggests that using RCA in web concrete not only enhances load capacity but also provides economic and environmental benefits compared to natural coarse aggregate (NCA).
- Load-deflection curves indicate that as the reinforcement ratio increases, the T-beams transition from flexural to shear behavior with rising aggregate replacement ratios.
- Shear cracks develop and intensify as the percentage of main reinforcement increases. Nonetheless, replacing NCA with RCA contributes to the growth and expansion of shear cracks, ultimately leading to shear failure as the predominant failure mode.
- A higher aggregate replacement ratio correlates with decreased ductility, particularly in T-beams with a high reinforcement ratio.
- Conversely, the increase in aggregate replacement enhances the stiffness of concrete T-beams, especially those with significant reinforcement. This effect may be attributed to the initial load resistance offered by recycled aggregates, which diminishes with increased loading.

Future research should focus on optimizing RCA proportions in SCC to achieve a better balance between workability and strength. It is essential to investigate the long-term durability of these materials, including their resistance to sulfate and acid attacks, corrosion of steel reinforcement, and chloride ion penetration. Additionally, exploring the effects of RCA on other structural elements, such as slabs and columns, will be crucial for a comprehensive understanding.

## Acknowledgment

The authors acknowledge that this study is supported by the University of Kirkuk and Al-Qalam University College, in Kirkuk, Iraq.

## References

- [1] Meko B, Ighalo JO, Ofuyatan OM. Enhancement of self-compatibility of fresh self-compacting concrete: A review. *Cleaner Materials*. 2021;1:100019. <https://doi.org/10.1016/j.clema.2021.100019>
- [2] Mikhaltchouk I, Eklund J, Forsman M. Barriers and facilitators for usage of self-compacting concrete-An interview study. *Inventions*. 2024;9:50. <https://doi.org/10.3390/inventions9030050>
- [3] Siddique R. *Self-compacting concrete: materials, properties, and applications*. Woodhead Publishing; 2019.
- [4] Shawais ZA, Abdulhaleem KN, Ahmed SH, Hamada HM, Mohammed VR. Influence of recycled coarse aggregate and steel fiber on the workability and strength of self-compacting concrete. *IOP Conf Ser Earth Environ Sci*. 2024; p. 012084. <https://doi.org/10.1088/1755-1315/1374/1/012084>
- [5] Mohammed VR, Abdulhaleem KN, Hamada HM, Humada AM, Majdi A. Effect of recycled aggregate concrete and steel fibers on the fresh properties of self-compacting concrete. *E3S Web Conf*. 2023; p. 02013. <https://doi.org/10.1051/e3sconf/202342702013>
- [6] Xiao J, Xiao J. *Recycled aggregate concrete*. Springer; 2018. <https://doi.org/10.1007/978-3-662-53987-3>
- [7] Sun C, Chen Q, Xiao J, Liu W. Utilization of waste concrete recycling materials in self-compacting concrete. *Resour Conserv Recycl*. 2020;161:104930. <https://doi.org/10.1016/j.resconrec.2020.104930>
- [8] Xiao J, Li L, Tam VW, Li H. The state of the art regarding the long-term properties of recycled aggregate concrete. *Struct Concr*. 2014;15(1):3-12. <https://doi.org/10.1002/suco.201300024>
- [9] Hamada HM, Jokhio GA, Al-Attar AA, Yahaya FM, Muthusamy K, Humada AM. The use of palm oil clinker as a sustainable construction material: A review. *Cem Concr Compos*. 2020;106:103447. <https://doi.org/10.1016/j.cemconcomp.2019.103447>
- [10] Hamada HM, Al-Attar A, Abed F, Beddu S, Humada AM, Majdi A. Enhancing sustainability in concrete construction: A comprehensive review of plastic waste as an aggregate material. *Sustain Mater Technol*. 2024;40. <https://doi.org/10.1016/j.susmat.2024.e00877>
- [11] Abed M, Nemes R, Tayeh BA. Properties of self-compacting high-strength concrete containing multiple uses of recycled aggregate. *J King Saud Univ Eng Sci*. 2020;32:108-14. <https://doi.org/10.1016/j.jksues.2018.12.002>

- [12] Bonoli A, Zanni S, Serrano-Bernardo F. Sustainability in building and construction within the framework of circular cities and European new green deal: The contribution of concrete recycling. Sustainability. 2021;13:2139. <https://doi.org/10.3390/su13042139>
- [13] Hamada HM, Shi J, Abed F, Humada AM, Majdi A. Recycling solid waste to produce eco-friendly foamed concrete: A comprehensive review of approaches. J Environ Chem Eng. 2023;11:111353. <https://doi.org/10.1016/j.jece.2023.111353>
- [14] Abdhaleem KN, Hamada HM, Majdi A, Yousif ST. Influence of palm oil fuel ash as agricultural waste on the environment and strength of geopolymer concrete. 2024.
- [15] Sasanipour H, Aslani F. Durability properties evaluation of self-compacting concrete prepared with waste fine and coarse recycled concrete aggregates. Constr Build Mater. 2020;236:117540. <https://doi.org/10.1016/j.conbuildmat.2019.117540>
- [16] Kapoor K, Singh S, Singh B, Singh P. Effect of recycled aggregates on fresh and hardened properties of self-compacting concrete. Mater Today Proc. 2020;32:600-7. <https://doi.org/10.1016/j.matpr.2020.02.753>
- [17] Hason MM, Mussa MH, Abdulhadi AM. Flexural ductility performance of hybrid-recycled aggregate reinforced concrete T-beam. Mater Today Proc. 2021;46:682-8. <https://doi.org/10.1016/j.matpr.2020.11.747>
- [18] You ZG, Wang XG, Liu GH, Chen HB, Li SX. Shear behavior of hybrid fiber-reinforced SCC T-beams. Mag Concr Res. 2017;69:919-38. <https://doi.org/10.1680/jmacr.16.00470>
- [19] Khtara AK, Khudhaira JA. Flexural behavior of reinforced concrete T-beam cast with self-compacting concrete incorporating recycled concrete aggregate. Muthanna J Eng Technol (MJET). 2018;6. <https://doi.org/10.18081/mjet/2018-6/210-221>
- [20] Fahmy MF, Idriss LK. Flexural behavior of large scale semi-precast reinforced concrete T-beams made of natural and recycled aggregate concrete. Eng Struct. 2019;198:109525. <https://doi.org/10.1016/j.engstruct.2019.109525>
- [21] Lec A, Malik MM, Ali AY. Flexural and shear behavior of reinforced concrete T-section beams composed of hybrid concrete. 2015.
- [22] Fang Z, Jiang H, Liu A, Feng J, Chen Y. Horizontal shear behaviors of normal weight and lightweight concrete composite T-beams. Int J Concr Struct Mater. 2018;12(1):1-21. <https://doi.org/10.1186/s40069-018-0274-3>
- [23] Marzoq ZH, Borhan TM. The behavior of hybrid-reinforced concrete T-beams exposed to the flexural moment. Asian J Civ Eng. 2020;21:1005-12. <https://doi.org/10.1007/s42107-020-00257-9>
- [24] ASTM C. 1084: Standard Test Method for Portland-cement content of hardened hydraulic-cement concrete. Philadelphia, USA; 1992.
- [25] Bakhrakh BA, Solodov A, Larsen O, Naruts V, Aleksandrova O, Bulgakov B. SCC with a high volume of fly ash content. MATEC Web Conf. 2017; p. 03016. <https://doi.org/10.1051/mateconf/201710603016>
- [26] Testing and Materials ASF. ASTM C136/C136M-19: Standard Test Method for Sieve Analysis of Fine and Coarse Aggregates. 2019.
- [27] Bibm C, ERMCO EE, EFNARC. The European guidelines for self-compacting concrete: Specification, production, and use. SCC European Project Group, EFNARC; 2005.
- [28] En B. 12390-3, Testing hardened concrete-Part 3: Compressive strength of test specimens. British Standards Institution. 2009; 22.
- [29] ASTM C. Standard test method for splitting tensile strength of cylindrical concrete specimens. ASTM International C. 2011; 496.
- [30] Rabi M, Shamass R, Cashell K. Structural performance of stainless steel reinforced concrete members: A review. Constr Build Mater. 2022;325:126673. <https://doi.org/10.1016/j.conbuildmat.2022.126673>
- [31] Arslan G, Cihanli E. Curvature ductility prediction of reinforced high-strength concrete beam sections. J Civ Eng Manag. 2010;16:462-70. <https://doi.org/10.3846/jcem.2010.52>
- [32] Rakhshanimehr M, Esfahani MR, Kianoush MR, Mohammadzadeh BA, Mousavi SR. Flexural ductility of reinforced concrete beams with lap-spliced bars. Can J Civ Eng. 2014;41:594-604. <https://doi.org/10.1139/cjce-2013-0074>
- [33] Abdul-Razzaq KS, Abdul-Kareem MM. Innovative use of steel plates to strengthen flange openings in reinforced concrete T-beams. Structures. 2018;16:269-87. <https://doi.org/10.1016/j.istruc.2018.10.005>
- [34] Etman EE, Afefy HM, Baraghith AT, Khedr SA. Improving the shear performance of reinforced concrete beams made of recycled coarse aggregate. Constr Build Mater. 2018;185:310-24. <https://doi.org/10.1016/j.conbuildmat.2018.07.065>